

CONF-93091971-2

FEMP-2293  
PAPER

RADON MEASUREMENTS AT THE FEMP

BY

L. M. Tomczak, R. D. Daniels, H. H. Glassey, W. G. Lohner,  
E. C. Ray, and J. A. Salesky, FERMCO\*

and

H. B. Spitz, University of Cincinnati

August, 1993

Fernald Environmental Restoration Management Corp\*  
Fernald Environmental Management Project  
P.O. Box 398704, Cincinnati, Ohio 45239-8704

For Presentation at the

The 1993 International Radon Conference  
Denver CO, September 20-23, 1993

RECEIVED

FEB 14 1994

OSTI

\*Fernald Environmental Restoration Management Corp. with the U.S. Department of Energy under Contract No. DE-AC05-92OR21972

**DISCLAIMER**

This report was prepared as an account of work sponsored by an agency of the United States Government. Neither the United States Government nor any agency thereof, nor any of their employees, makes any warranty, express or implied, or assumes any legal liability or responsibility for the accuracy, completeness, or usefulness of any information, apparatus, product, or process disclosed, or represents that its use would not infringe privately owned rights. Reference herein to any specific commercial product, process, or service by trade name, trademark, manufacturer, or otherwise does not necessarily constitute or imply its endorsement, recommendation, or favoring by the United States Government or any agency thereof. The views and opinions of authors expressed herein do not necessarily state or reflect those of the United States Government or any agency thereof.

MASTER

DISTRIBUTION OF THIS DOCUMENT IS UNLIMITED

gdc

## **RADON MEASUREMENTS AT THE FEMP**

L. Tomczak, R. Daniels, C. Dennis, H. Glassey, W. Lohner, E. Ray, and J. Selasky  
Fernald Environmental Restoration Management Corporation  
Cincinnati, OH

H. Spitz and K. Roush  
University of Cincinnati  
Cincinnati, OH

### **ABSTRACT**

Environmental radon monitoring activities at the DOE Fernald Environmental Management Project (FEMP) have been conducted extensively since the early 1980s. Monitoring has been conducted at ambient concentration levels ( $< 1$  pCi/L Rn-222), inside buildings, and at significantly elevated levels (hundreds of thousands pCi/L Rn-222) within the K-65 silos that store concentrated radium bearing wastes. The purpose of this paper/presentation is to present and discuss some of the difficulties encountered/solutions (e.g. reliability, detection limits, affects of environmental factors, data transfer, etc.) that have been discovered while taking measurements using both alpha track-etch passive integrating detectors and alpha scintillation real-time detectors. A short summary and conclusion section is provided following each topic presented.

### **INTRODUCTION**

The Fernald Environmental Management Project (FEMP), formerly the Feed Materials Production Center (FMPC) a uranium metals processing facility, is today the focus of extensive environmental restoration activities. Owned by the U.S. Department of Energy (DOE), the site and surrounding areas are closely monitored for contamination and after data evaluation remedial techniques are developed accordingly.

In the late 1940s, after evaluating several locations, the government selected a 425 hectare (1,050-acre) site about 27 km (17 miles) northwest of downtown Cincinnati, Ohio, as the site for a new production facility. Ground was broken on May 1951, and the first uranium derby was produced at the site's Pilot Plant in October 1951. The major portion of construction was completed by 1954. For many years much of the uranium processed was slightly enriched - up to 2% uranium-235. The majority of the uranium processed in recent years was depleted in the uranium-235 isotope - less than the natural 0.71%.

Two reinforced concrete storage silos were constructed in 1951 and 1952. Each silo is approximately 24.4 m (80 ft.) in diameter and 8.3m (27 ft.) high, yielding a volume of  $3540 \text{ m}^3$  ( $125,000 \text{ ft}^3$  or one million gallons). The silos were constructed to provide storage for process residues from the refining of high grade pitchblende ores from South Africa. These residues, known as K-65 residues, were received between 1952 and 1958. Presently, the combined inventory of waste material in the two K-65 silos is estimated at  $5523 \text{ m}^3$  ( $195,000 \text{ ft}^3$ ). In 1991, a bentonite sealant was placed over the residues to reduce the amount of radon emitted into the headspace.

Production was suspended in July 1989. In October 1990, the DOE transferred management responsibility for the site from its Defense Programs organization to the Office of Environmental Restoration and Waste Management. In February 1991, DOE announced its intention to formally end production and submitted a closure plan to Congress, becoming effective in June 1991. Subsequently, in August 1991, the site was renamed the Fernald Environmental Management Project in accordance with the new mission.

## ENVIRONMENTAL RADON AIR MONITORING AT THE FEMP

The FEMP has monitored radon levels routinely since the early 1980s. It is believed that the principal source of radon emissions from the FEMP is currently the K-65 silos due to their radon-emitting ore residues. Radon escapes through tiny cracks, and access ports, on top of the K-65 silos. To ensure emissions are monitored as efficiently as possible, radon concentration measurements are taken in the air at several locations: immediately adjacent to the silos, points at the FEMP facility fence line, and in each silo's headspace. Waste pits 1, 2, 3, and 4 have been monitored and are considered minor sources of radon. Waste Pit 5 is a potential source of radon emissions when not covered with water. Waste Pit 6 is not considered a source of radon since very few radium-bearing materials are contained within it.

It is DOE's objective to conduct activities at its facilities such that radiation exposures to members of the public are maintained As Low As Reasonably Achievable (ALARA). Therefore, DOE facilities monitor all releases applicable to site activities. Since the FEMP stores radium-bearing materials onsite, radon concentrations in the atmosphere above facility surfaces or openings are regulated by DOE Order 5400.5. When added to background levels, these concentrations must not exceed the following limits:

- 100 pCi/L at any given point
- An annual average concentration of 30 pCi/L over the facility site,
- An annual average concentration of 3 pCi/L at or above any location outside the facility site, or
- Flux rates greater than 20 pCi/m<sup>2</sup> per second from the storage of radon producing wastes.

NESHAP subpart Q also has a flux-rate requirement, but will not be applicable until on-going remedial actions have been conducted and the final remedial action to abate the radon emission problem has taken place. These actions are enacted to comply with the requirements of the Federal Facility Compliance Agreement/Federal Facility Agreement (FFCA/FFA). Therefore, all actions related to the control and abatement of radon-222 at the FEMP are performed in cooperation with USEPA.

### RADON MONITORING METHODOLOGIES

To determine radon concentrations in the environment, the FEMP uses two monitoring systems for the alpha particles produced as radon gas decays: alpha track-etch detectors and real-time alpha scintillation detectors.

The alpha track-etch detector consists of a filtered cup surrounding a plastic chip, the molecules of which are damaged when contacted by alpha particles. The filter acts as a diffusion barrier, preventing airborne alpha particles and radon daughters from entering. Therefore, only radon atoms are free to diffuse into the cup. When alpha particles from radon and its daughters interact with the plastic, ionization damage produces latent tracks. These tracks can be visualized by chemical treatment or electrochemical etching. The number of etches or tracks in the material is equal to the number of alpha particles that have reached the plastic. This number can then be related to the average concentration of radon in the cup.

Real-time alpha scintillation monitors record ambient environmental radon concentrations on an hourly basis. They detect alpha particles by using a scintillation cell. They operate in the passive mode, allowing air to diffuse into the detector through a foam barrier. Radon present in the diffused air will decay along with its alpha-emitting daughters, and the alpha particles strike the sensitive ZnS scintillator which lines the interior of the cell. Each interaction produces light pulses, which are amplified by a photomultiplier tube and then are counted. It takes about a half-hour to achieve the same radon gas equilibrium inside the detector as is present in the surrounding air.

### RADON MONITORING RESULTS

The following accounts describe some of the difficulties encountered in various radon monitoring activities and resolutions to the problems encountered while using alpha track-etch and real-time scintillation detectors in the sampling program.

### Alpha Track-etch Detectors

Environmental data has been collected for several locations: at the site boundary, background locations, area residences, and at locations adjacent to the silos and in the predominant wind direction relative to them. Together with limited indoor building monitoring, a total of 65 locations are monitored. The detectors are changed quarterly and provide long-term integrated radon measurements. The typical monitoring setup involves the use of three or four cups depending upon the location.

In the past there have been occasions where substantial differences in radon concentration values have been recorded for cups at the same location. To determine the precision and reliability of the alpha track-etch cups, an experiment using replicate measurements was designed to assess the variability of the measurements at a particular outdoor exposure level. For this study, the northeast corner of the K-65 silo fence line was chosen to provide the highest onsite concentrations (typically > 1 pCi/L), the area near the meteorological tower to represent typical onsite concentrations, and an offsite location which would be typical of background radon levels with no influence from sources at the FEMP.

The measurement period was approximately 3 months (from December 1992 until mid-March 1993). Twenty cups were used at both the K-65 silo location and the meteorological tower, and 21 cups were used at the offsite location. The cups at each location were placed only inches from each other to ensure they were measuring the same ambient radon concentrations. The following equation was used to determine the sample number at each location:

$$n = \left( \frac{z \cdot \sigma}{e} \right)^2 \quad (1)$$

n = number of detectors at each measurement location

$\sigma$  = 0.2  
(This value of standard deviation was adopted based on the evaluation of previous routine environmental radon measurement data collected).

e = 10%  
(This value of expected outlier frequency was also based on the evaluation of previous routine environmental radon measurement data collected).

z = 1.645  
(This value was selected from the normal curve to obtain a 95% confidence interval for the measurements).

Analysis of the data yielded the following results (based on net count data):

Table 1. Outlier Data

LOCATION	DATA BELOW THE MINIMUM SENSITIVITY OF THE DETECTOR	OUTLIERS
NE Corner of Silo Area	0 %	20 % (upper extreme)
Met. Tower	45 %	0 %
Background	100 %	5 % (lower mild)

As a quality assurance test, seven cups were placed within an aged air atmosphere (also for three months), thus providing a radon-free environment. Measurement of these cups yielded two false positives, an error rate of 29%.

## SUMMARY AND CONCLUSIONS

The detectors appear to meet the performance criteria when placed outdoors for a period of three months in areas having an elevated radon concentration. At lower concentrations the reliability becomes more questionable when exposure is for the same time frame. The frequency of false positive results observed in the quality control process using a radon-free environment exceeded expectations.

Perhaps, more precise results from the alpha track-etch detectors in measuring low-level ambient radon concentrations could be obtained by increasing the exposure period. Further investigation of their response in low level environmental applications is required.

### Real-time Scintillation Detectors

Fifteen continuous radon monitors have been installed at both on-site and off-site locations. On-site outdoor locations were selected to provide representative measurements that are either close to the sources of emission (K-65 silos) or near buildings and areas where production occurred. Several monitors measure radon at the FEMP fence line and at two background locations (a minimum of 13 km from the project) with one located in the opposite direction of the prevailing wind. In addition to the routine environmental radon monitoring programs, real-time alpha scintillation detectors are also used to monitor radon head space concentrations within the K-65 silos.

### K-65 Silo Headspace Monitoring

Grab sampling of the K-65 silo headspace has historically indicated radon concentrations in excess of  $3 \times 10^7$  pCi/L. In an effort to reduce the emanation of radon gas from the radium-bearing wastes (and therefore reduce emanations from the silos, themselves) the residues were covered with a 1.2 m (4 ft.) thick layer of bentonite clay in 1991. Modeling projected the bentonite covering should decrease radon equilibrium concentrations to less than  $4 \times 10^6$  pCi/L. This value, in part, established the criteria for measuring the success of the covering. Continuous radon monitoring of the silo void, in lieu of periodic gas or progeny sampling, was considered the best means of assessing the bentonite effectiveness. This led to the development of the Data Logging System (DLS). The DLS is designed to monitor and provide output for the physical and radiological parameters which affect radon emissions and the integrity of the bentonite: radon concentration, temperature, pressure, and humidity.

The continuous radon measurement portion of the DLS system is based on using an alpha-scintillation monitor coupled to a modified 151 ml flow-through scintillation cell. Silo air is drawn through the cell by an external pump at a nominal flow rate of 300 ml/min. The air sample is pumped through a desiccant column, a prefilter for progeny removal, and then the scintillation cell. The monitor is set for continuous counting at 5 minute intervals to provide local data output via an installed printer. The pulsed output is accumulated and sent to a microcomputer for data reduction and reporting. The desiccant columns, prefilter, pulse accumulators, radon monitor, and cell assemblies for each silo sampling system are located within a weather-proof enclosure in close proximity to the silos. Provisions were made within the enclosure to allow for static sample acquisition in parallel with the continuous system. This allows comparisons of differing sampling methods from the same stream. The main computer system is located outside the silo exclusion area, and a remote terminal is located near the site boundary.

In adapting the monitoring system for this application, a problem in cell calibration was encountered. A loss of counting efficiency corresponding to an increased count rate is an unavoidable occurrence when determining radon concentrations by scintillation. This phenomenon is commonly referred to as "pulse overlap" and is related to the photomultiplier tube's ability to discern events. At environmental levels, this variance is not limiting and a single static calibration representing the expected range of concentrations will suffice. The silos require monitoring over a wide range of elevated radon levels, lending to large errors in radon calculations if single point calibration efficiency is used. For example, a scintillation cell with a typical 75% counting efficiency as determined with a calibration concentration of  $3.0 \times 10^3$  pCi/L exhibited an efficiency of 52% for a radon concentration of  $2 \times 10^6$  pCi/L. This would result in a 70% underestimate of true radon concentration if the initial calibrated efficiency value is used in computations. Reducing the amount of scintillation material in the scintillation cell acts to counter the rate of

decreased efficiency, but at the cost of cell sensitivity. A cell coated to provide a nominal efficiency of 2% was initially tested for the DLS. During calibration, the cell demonstrated little change in efficiency for concentrations up to  $8 \times 10^6$  pCi/L. Although initially promising when placed in the field, the cell failed to provide an adequate signal for the DLS when monitoring radon concentrations below  $10^5$  pCi/L. Experimentation led to the development of a modified 20% efficient cell. The active cell surface area was selected to provide an accurate determination of radon concentration over the expected range of  $3.0 \times 10^5$  pCi/L to  $4.0 \times 10^6$  pCi/L.

Given the wide range of concentrations found in monitoring the silos, some variation in efficiency is expected. In order to minimize the error associated with this anomaly, a method for estimating counting efficiency based on the scintillation rate was developed. The observed decrease in efficiency due to pulse overlap appears exponential and, as such, should be readily predicted. Empirical data was gathered from calibration records for a series of six test scintillation cells. The test cells were coated with the scintillation material to provide a nominal 20% counting efficiency for radon in equilibrium. Counting efficiencies were then plotted for each cell at ten differing concentrations, ranging from  $3.0 \times 10^5$  pCi/L to  $7.5 \times 10^6$  pCi/L. The known concentrations were generated under controlled conditions at the vendor calibration facility. These data were assembled and used to predict efficiency from a fitted curve by exponential regression. An example of this data is included in Figure 1. All tests performed show in excess of 90% correlation between predicted efficiency values and actual values.

#### Adjusting Continuous Hourly Measurements of Radon for Decay of Radon Daughter Products

The hourly average radon concentration determined by a passive alpha scintillation continuous radon monitor is a function of the net counts per hour and the instrument's calibration factor. Improved accuracy can be achieved by increasing the observation interval from 1 to 4 hours, and by applying a correction factor for the ingrowth of radon decay products in the detector. Figure 2 compares data averaged in one hour intervals as opposed to data averaged every four hours.

Busigin et. al. developed a forward-marching data analysis procedure to correct each 4 hour integrated measurement for the lag associated with the ingrowth of the radon daughter products. The total number of counts observed within a counting interval depends on three factors: (1) the radon concentration during the interval, (2) the activity of the daughters deposited during the interval, and (3) the activity of the daughters deposited in previous intervals. Since the concentration of radon in outdoor air is not constant and exhibits a large, diurnal-like variation, a correction must be applied to hourly measurements to account for the lag in detector response associated with the build up and decay of radon daughter products. Their method accounts for the production, deposition, and decay of radon daughters as a function of time to correct the hourly radon measurement. The radon concentration in any interval can be calculated by the following equation:

$$C_{Rn,j} = \frac{Y_j}{0.037V\alpha\xi\tau} - h_1\left(1 - \frac{1}{\alpha}\right)C_{Rn,j-1} - h_2\left(1 - \frac{1}{\alpha}\right)C_{Rn,j-2} - \dots - h_i\left(1 - \frac{1}{\alpha}\right)C_{Rn,j-i} \quad (2)$$

Where:

- $C_{Rn,j}$  is the predicted average concentration in counting interval j (pCi/L)
- $Y_j$  is the counts of alpha disintegrations in counting interval j (counts)
- $V$  is the volume of the sensitive portion of detection (L)
- $\alpha$  is a constant that depends on the length of the counting interval, the half lives of  $Rn^{222}$ ,  $Po^{218}$ ,  $Pb^{214}$ , and  $Bi^{214}$ , and the detection efficiencies for  $Rn^{222}$ ,  $Po^{218}$ , and  $Po^{214}$
- $\tau$  is the detection efficiency for  $Rn^{222}$
- $\xi$  is the length of the counting interval (sec)
- $h_j$  are constants that depend on the number of previous counting intervals, i, the length of the counting interval, and the half lives of  $Rn^{222}$ ,  $Po^{218}$ ,  $Pb^{214}$ , and  $Bi^{214}$
- $i$  is the index of the number for the previous counting interval

Improved precision without sacrificing accuracy is easily obtained by increasing the duration of the count interval from 1 to 4 hours. To further increase the precision, the forward-marching algorithm is applied to the four hour continuous radon measurement to account for the lag in the daughter product buildup. The actual radon concentration will be lower than that recorded by the instrument without the correction for decay product ingrowth.

### Statistical Analyses of Real-time Environmental Radon Monitoring Results

Statistical analyses of radon measurement results were conducted to determine what contribution, if any, the radon emanations from the radium-bearing materials within the silos makes to the ambient radon concentration on and around the FEMP. This study adopted the nested and nested factorial classification models to eliminate the random effect associated with selecting individual monitoring locations so that the radon concentrations in different areas of the site could be evaluated. The site was divided into four general areas: (1) the boundary or perimeter, (2) the production and administration area, (3) the waste storage area, and (4) an offsite location approximately 13 km from the FEMP to represent the natural radon background.

Data from fifteen continuous radon monitors measuring in hourly intervals between February 1991 and 1992 were used to determine the radon concentration in these four areas. Measurement results from an individual monitor are best described by the log-normal distribution. A series of contrast tests were performed which demonstrate that the radon concentrations in all of the areas, excluding the silo area, are statistically equal to the natural background. This analysis also confirms that the bentonite clay sealant, applied to the surface of the residue in the silos, appears to have a significant effect in reducing radon emissions.

The choice of monitoring locations within an area may affect the outcome of the analysis if the random effect associated with choosing a sampling location cannot be eliminated. The nested classification method was adopted to partition the variance of the measurement results so that the individual components of the variance could be evaluated. The terms "Location (Loc)" (which is nested within an area) and "Area" are the only two factors considered in the application of this statistical model. The model is shown in the following equation:

$$\ln(Rn)_{ijk} = \mu + (Area)_i + Loc(Area)_{j(i)} + \epsilon_{ijk} \quad (3)$$

Assuming that the difference of atmospheric conditions between February 1991 and 1992 does not greatly affect the radon measurement, the only factor that would make a difference in the measurement results in the identical areas would be the application of the bentonite clay barrier in November 1991. A cross factor, Year (Yr), which accounts for the sealant, is added into the model in the previous equation and produces a nested factorial model as shown in the equation below (Li 93):

$$\ln(Rn)_{ijkl} = \mu + (Area)_i + Loc(Area)_{j(i)} + (Yr)_k + (Area * Yr)_{ik} + [Yr * Loc(Area)]_{jk(i)} + \epsilon_{ijkl} \quad (4)$$

The subscript k represents the corresponding time in the year of 1991 and 1992 and l is the measurement replication. The factor Yr has a fixed number of levels, 1991 and 1992; thus, it is a fixed factor.

An analysis of both models was performed using Analysis of Variance (ANOVA), and multiple contrasts between the locations and years were performed. Figure 3 depicts the relationship between the locations and the time separation of the data.

Based on the results of the statistical analyses performed as summarized in this paper, it can be concluded that: (1) there is no significant evidence to show that radon emission from the silo area makes any contribution to the environmental radon concentration, and (2) the bentonite clay barrier applied to the material in the silo is effective in reducing the flux of radon from the silo and accounts for the observed reduction in the measured radon concentration in the silo area.

### Radon Distribution Data

It is reasonable to expect that the diurnal cycle (24 hour period) observed for both inside and outside average onsite radon concentrations shown in Figure 4, is related to some atmospheric condition which exhibits the same diurnal trend. The atmospheric condition which best fits this pattern is known as the nocturnal inversion. This inversion forms due to nightly radiation cooling of air layers next to the earth's surface, while layers above remain warmer.

Inversions form whenever there is cooling below or heating above a given layer of air, and are related to both the atmospheric stability and lapse rate. The lapse rate is the rate of change of temperature with height. The lapse rate is about -9.8°C/km for dry air, and is referred to as the dry adiabatic lapse rate. Any parcel of unsaturated air

(imagine a balloon filled with air) which is lifted or rises, expands and cools at this rate. The term adiabatic is used because heat is neither absorbed from nor released to the surrounding air. Under this condition the atmosphere is considered neutral. Typically, however, the atmosphere is either stable or unstable. In the former case, the temperature profile changes at a rate slower than  $-9.8^{\circ}\text{C}/\text{km}$ . Under these conditions, any rising air will be cooler than the surrounding air. Consequently, there is no buoyancy to the air parcel when compared with its environment (the surrounding air) and it begins to sink. For an unstable air mass, the temperature profile would change at a rate faster than  $-9.8^{\circ}\text{C}/\text{km}$ . Any rising air parcels are warmer than the surrounding air. In this case a buoyancy force exists and it continues to rise. Thus, in a stable atmosphere, buoyancy forces oppose vertical motion, and in an unstable atmosphere, buoyancy forces enhance vertical motion (Se 86). Stating it another way, stable conditions in the atmosphere restrict mixing, and unstable conditions increase mixing.

Figure 5 shows the average hourly temperature difference between two levels on the Fernald Meteorological Tower. Data was taken during the same period as the radon data used for this study. The upper level is located at 60 m and the lower level at 10 m. The graph shows the difference between the 60 and 10 m temperatures. For use as a reference, the average and dry lapse rates for a 50 m height difference were included. Therefore, values greater than about  $-0.5^{\circ}\text{C}$  (dry air) indicate a stable layer, i.e. little or no mixing near the earth's surface, and values less than about  $-0.5^{\circ}\text{C}$  indicate an unstable layer, i.e. much mixing.

Comparing the plotted radon data to the temperature differences, it is clear that there is a strong relationship between the increase in radon levels and the presence of the nocturnal inversion. For this study, as the inversion starts to form around 5 pm, the atmosphere becomes stratified, or stable, and acts as a cap, much like the inversions which trap pollution in major metropolitan areas. Hence, the radon levels rise and peak around 8 am, then decrease as the inversion breaks down. Due to seasonal changes, the inversion formation/breakdown time changes. Also, note the small lag time in the radon concentrations, due to the transition periods between inversion and non-inversion conditions, and the apparent slow release rate of radon from sources around the FEMP site.

The major source of radon at the FEMP site is the K-65 Silos, located on the western side. Trailer 45 is located between the K-65 Silos and the Administration Building. From Figure 4 one can see that radon concentrations vary from a ratio of about 3:1, to 2:1, between the maximum and minimum radon values. Also, as expected, radon levels decrease at greater distances from the silos.

Many other inversions can form, some of which last for shorter or longer periods than overnight. Frontal inversions form at the boundary of air masses because of the differences which can exist in the properties of the two air masses, e.g. temperature and humidity. Advective inversions can form when warmer air moves over a layer of cooler air or a cooler surface (Se 86). Subsidence inversions form when air at higher levels in the atmosphere sinks and warms due to the compression air parcels undergo during this process. This inversion can form easily in the winter under strong high-pressure systems, often lasting for days. Consequently, if a subsidence inversion is strong and low enough, one might expect radon levels at the FEMP to increase as long as the inversion exists.

Knowing the conditions under which inversions form implies that forecasts could be made on the time that radon concentration levels might increase. In addition, if some idea of the rate at which the radon is released could be made, then some prediction of the magnitude of radon concentrations might be possible. Also, data could be accumulated and processed to give a statistical average of the concentration for a given type of inversion. Then any other radon data obtained for study during major release events could be corrected for the diurnal changes in concentration.

#### Electronic Radon Data Transfer

Electronic Data Transfer is a practice that results in an overall improvement in quality assurance of collected data. It reduces the manpower normally required in manual data entry while increasing the quality of the data transferred. The application of this practice can enhance any data collection program involving instruments with electronic memories and signal output. The use of such practices assist in complying with Quality Assurance requirements under ASME, EPA, NQA-1, RCRA, CERCLA, and DOE Order activities.

Data from real-time monitors is typically configured to print data to a tape. However data can be sent from the real-time monitor to a portable hand-held computer. Data are recorded and stored on a 128 K-byte RAM card and later transferred to a microcomputer database in electronic files for analysis. The advantage of this system is twofold: (1) Data entry errors are eliminated and (2) extensive data entry time is eliminated.

There are essentially two steps in the electronic data transfer process. The first is the transfer of electronic data file from the real-time monitor to a RAM card by using a handheld computer, while in the field. The second step is the transfer of field data from the RAM card to an electronic data file back at the office onto the hard drive of a microcomputer (He 91). The hardcopy data tape and the electronic files are then transferred to a data previewer, and then to an independent group that produces the environmental reports. This activity eliminates data entry errors. Following is a list of equipment that is needed to complete the electronic data transfer from the AB-5 Pylon to a personal IBM disk operating system computer.

- Pylon AB-5 Radon Monitor
- Pylon Model CI-55 Computer Interface
- CPRD (radon detector) or a 300A Lucas cell
- DB15 Female A/B Switch Box
- DB15 3 foot M.F. Transfer Cable
- DB15 M.M. Gender Changer
- 128 K-byte RAM carddrive linked to PC
- Pylon Model PPT-1 Printer
- HPF1001a Connectivity Pack
- HP95LX Hand Held Computer
- DB15 3 foot M.M. Transfer Cable
- DB25/9 M.M. Gender Changer
- HP F1002A 128 K-byte RAM card

Using the electronic transfer scheme described allows for easy collection of radon data into user-friendly electronic files for further processing. Once transferred to disk, spreadsheet programs can be used to preview the data by the individual assigned to quality assurance and data validation. Data analysis requires separating the data into different columns using the spreadsheet's parsing function (this data translation is required regardless of the software programs utilized, and should be found in any software programs capable of handling ASCII). A check of data will then need to be conducted to confirm that the data was correctly transferred and that all data points were valid observations.

#### ACKNOWLEDGEMENTS

The authors wish to thank the following FERMCO personnel who have provided data or assistance in the preparation of this paper: S. Berry, J. Gore, J. Smith, A. Snyder, F. Emerich, K. Nilsson, and the University of Cincinnati students L. Dai, N. Liu, and S. McGimpsey.

#### REFERENCES

- Liu, N., et.al., Statistical Analysis of Real-time, Environmental Radon Monitoring Results at the Fernald Environmental Management Project, *Environmental Health Physics: Proceedings of the Twenty-sixth Midyear Topical Meeting of the Health Physics Society*, Columbia Chapter of the Health Physics Society, 1993.
- Seinfeld, J.H., *Atmospheric Chemistry and Physics of Air Pollution*, John Wiley & Sons, New York, N.Y., 1986.
- HP 95LX User's Guide*, Hewlett-Packard Co., Corvallis, Or., 1991.

THIS PAPER WAS PREPARED AS AN ACCOUNT OF WORK SPONSORED BY AN AGENCY OF THE UNITED STATES GOVERNMENT. REFERENCE HEREIN TO ANY SPECIFIC COMMERCIAL PRODUCT, PROCESS, OR SERVICE BY TRADE NAME, TRADEMARK, MANUFACTURER, OR OTHERWISE DOES NOT CONSTITUTE OR IMPLY ITS ENDORSEMENT, RECOMMENDATION, OR FAVORING BY THE UNITED STATES GOVERNMENT OR ANY AGENCY THEREOF. THE VIEWS AND OPINIONS OF AUTHORS EXPRESSED HEREIN DO NOT NECESSARILY STATE OR REFLECT THOSE OF THE UNITED STATES GOVERNMENT, OR ANY AGENCY THEREOF OR FERNALD ENVIRONMENTAL RESTORATION MANAGEMENT CORPORATION, ITS AFFILIATES OR ITS PARENT COMPANIES.

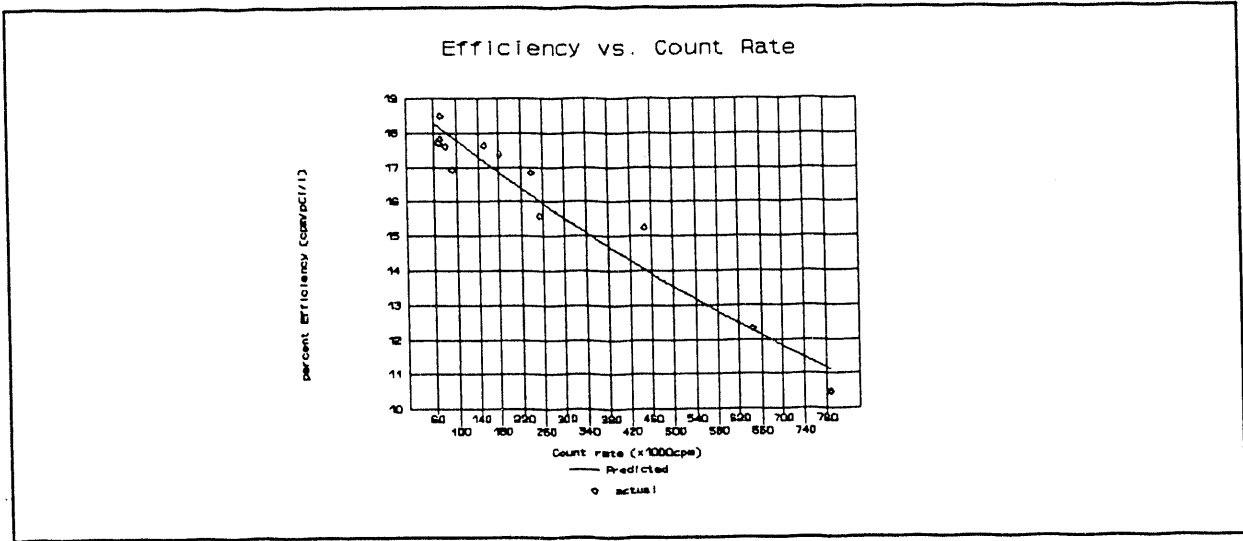


Figure 1. Scintillation Cell Efficiency vs. Count Rate

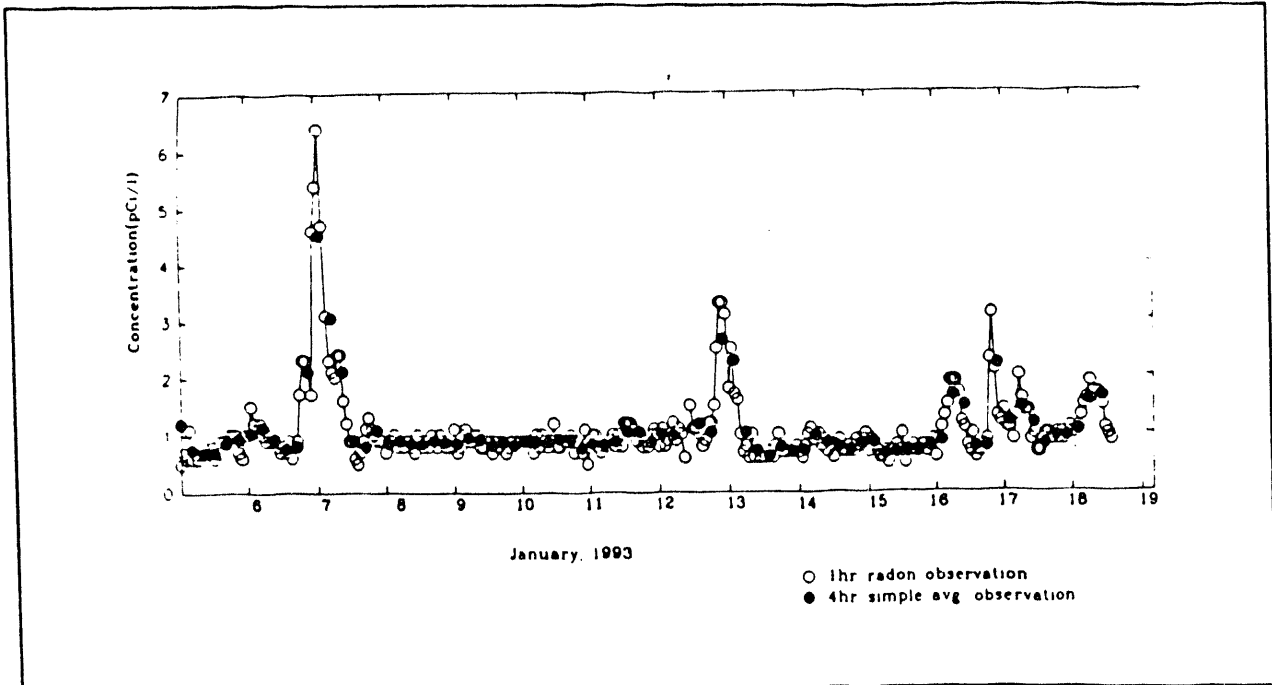


Figure 2. Comparison of One-hour and Four-hour Counting Interval

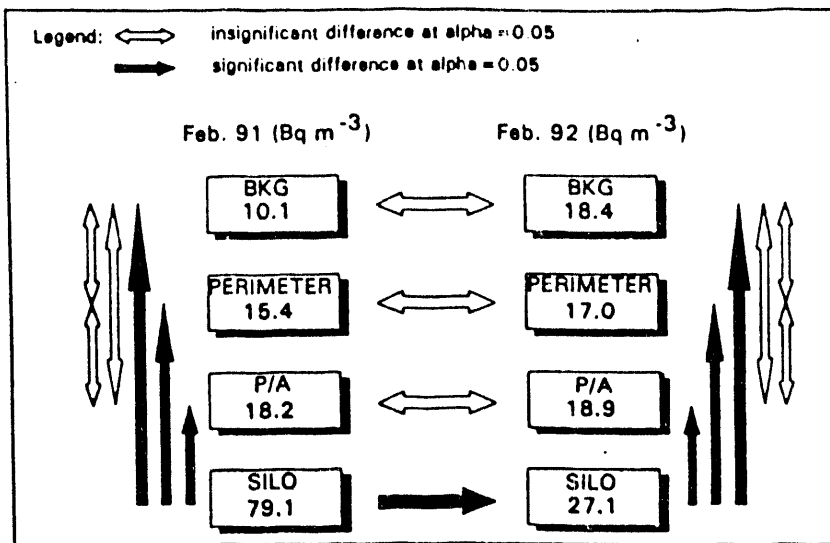


Figure 3. Summary of Statistical Tests

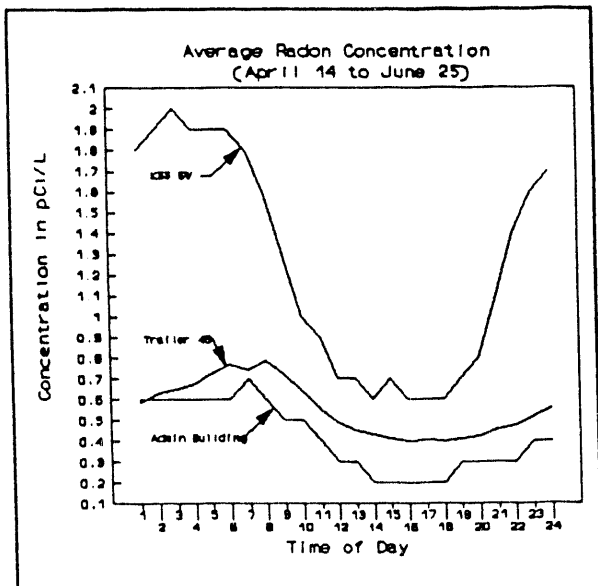


Figure 4. Average Radon Concentration

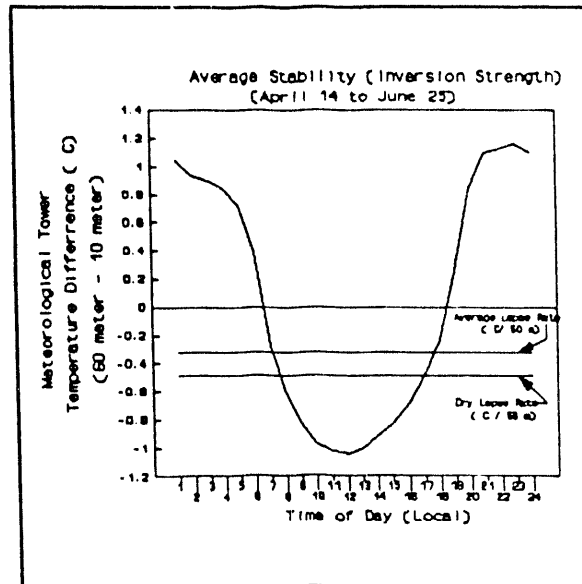


Figure 5. Inversion Strength

**END**

**DATE**

**FILMED**

**3/15/94**